Nonlinear tracking control of a two link oil palm harvesting robot manipulator

Ramin Shamshiri[1*], Wan Ishak Wan Ismail[2]

(1. *Department of Agricultural and Biological Engineering*, *University of Florida*, *Gainesville*, *FL* 32611, *USA*;
2. *Department of Biological and Agricultural Engineering*, *Universiti Putra Malaysia*, *Serdang*. *Selangor Darul Ehsan*, *Malaysia*)

Abstract: Automated harvesting of oil palm trees requires research and development efforts in several robotics areas, including manipulator control. The objective of this paper was to apply nonlinear Lyapunov based control method for joint angles tracking of a two-link oil palm harvesting robot manipulator with uncertain system parameters. Four different controllers, including exact model knowledge, adaptive, sliding mode control and high gain feedback control were proposed and simulated. Stability analyses were performed for each case in the absence and presence of bounded disturbance. The controllers were then compared against each other based on their performances and control efforts.

Keywords: harvesting robotics, oil palm, nonlinear control, manipulator control, Lyapunov method
DOI: 10.3965/j.ijabe.20120502.002

Citation: Shamshiri R, Wan Ishak W I. Nonlinear tracking control of a two link oil palm harvesting robot manipulator. Int J Agric & Biol Eng, 2012; 5(2): 9－19.

1 Introduction

Robotic technology is one of the fastest growing fields in the modern agriculture. Automated methods for harvesting, collection and transportation of agricultural products are demanded in leading producing countries to ensure long-term viability of their production under the increasing economic pressures. While studies on the development of robots for agricultural application such as robotic transplanting of tomato and strawberry in greenhouse environments are underway, few agricultural manipulator developments have utilized appropriate performance measured in configuring robotic manipulators for specific tasks[1]. This is mainly due to the highly variable environments in which agricultural robots are required to operate and perform dexterous agricultural task such as tree fruit removal.

Robots for harvesting of citrus fruits, cucumber, tomato and grape have been used in fields and greenhouse productions[2-7]. Researchers in the area of agricultural robotics are now challenged to develop electromechanical systems that allow for the exact placement of robot end-effectors. An important problem with most of the proposed controllers is that they do not consider the fact that the input command may require more torque than its physical possible. In the other words, when the actuator constraints are exceeded, hard nonlinearities that are not included in the dynamic model are encountered. Several robotic researchers have focused on the development of controllers based on more accurate models in an attempt to increase the performance of robot manipulator systems. For example, nonlinear control for adaptive regulation of robot manipulators with uncertain kinematics and dynamics are discussed in a number of literatures[8-13].

The objective of this work was to apply nonlinear Lyapunov based method to control joint angles in a two

Received date: 2010-09-08 **Accepted date:** 2012-05-03
Biography: Wan Ishak Wan Ismail, Professor, Email: wiwi@eng.upm.edu.my.
***Corresponding author: Ramin Shamshir,** Department of Agricultural and Biological Engineering, University of Florida, Gainesville, FL 32611, USA. Tel: 352-392-1864; Email: ramin.sh@ufl.edu.

link robot manipulator for harvesting oil palm. Four nonlinear controllers, including exact model knowledge (EMK), adaptive, sliding mode controller (SMC) and high gain feedback controller were designed and simulated to track a desired trajectory given by q_d = [cos(t) cos(t)]^T with uncertain system parameters (except the EMK controller whose system was exactly described), and in the absence and presence of bounded disturbances that are assumed to be modeled by τ_d=[2sin(t) 0.5sin(t)]^T. The Lyapunov stability analysis for each controller was performed and simulated to show how the bounded disturbances affect the stability of the system. Finally, the controllers were compared against each other based on their performances and control efforts.

2 Dynamic model and properties of the oil palm harvesting manipulator

The dynamic model for the tow-link robot system shown in Figure 1 can be written using the Euler-Lagrange formulation described by Spong et al.[14] as follows:

$$M(q)\ddot{q} + V_m(q,\dot{q})\dot{q} + f_d\dot{q} + \tau_d(t) = \tau \quad (1)$$

where, $M \in R^{2\times2}$ is the inertia matrix, $v_m \in R^{2\times2}$ denotes the centripetal-Coriolis matrix, $f_d \in R^2$ denotes friction, $\tau_d(t)$ is a general nonlinear bounded disturbance assumed to be modeled by τ_d=[2sin(t) 0.5sin(t)]^T, τ_t represents the torque input control vector and $q(t)$, $\dot{q}(t)$, $\ddot{q}(t)$ denote the link position, velocity, and acceleration vectors, respectively. The robot dynamic model given by Equation (1) has the following properties that will be used in the control development and analysis.

The inertia matrix $M(q)$ is symmetric and positive definite (PD) and satisfies the inequality in Equation (2) $\forall y(t) \in R^n$

$$m_1 \| y \|^2 \le y^T M(q) y \le \bar{m}(q) \| y \|^2 \quad (2)$$

where, $m_1 \in R$ is a known positive constant, $\bar{m}(q) \in R$ is a known positive function, and ||.|| denotes the standard Euclidean norm.

If $q(t)$, $\dot{q}(t)$ are bounded ($\in L_\infty$), then the first and second partial derivative of the elements of $M(q)$ and $V_m(q,\dot{q})$ with respect to q and the first and second partial derivative of the elements $V_m(q,\dot{q})$ and f_d with respect to $\dot{q}$ exist and are also bounded.

The time derivative of the inertia matrix and the centripetal Coriolis matrix satisfy the following skew symmetric relationship:

$$r^T\left(\frac{1}{2}\dot{M}(q) - V_m(q,\dot{q})\right)r = 0 \quad \forall r \in R^n \quad (3)$$

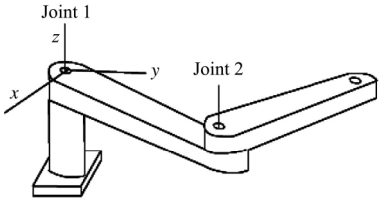

a. Schematic diagram of the oil palm harvesting robot manipulator

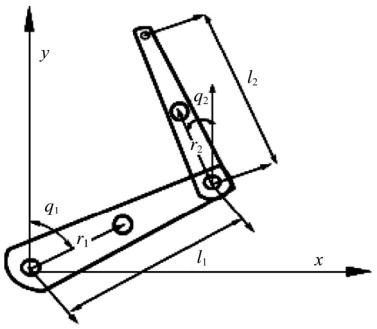

b. Top view

Figure 1 Dynamic model for the tow-link robot system

3 Control design and stability analysis

The control objective was to design controller for the oil palm robot manipulator model to simulate tracking of a desired joint space trajectory given by q_d = [cos(t) cos(t)]^T. We quantified the control objectives by defining the link position tracking error $e(t)$ and filtered tracking error $r(t)$ as follows.

$$e(t) = q - q_d \quad (4)$$

$$r(t) = \dot{e} + \alpha e \quad (5)$$

where, α is a positive diagonal gain matrix. The development of the controllers is based on the assumptions that $q(t)$ and $\dot{q}(t)$ are measurable, $M(q)$, $V_m(q,\dot{q}), f_d$ and $\tau_d(t)$ are unknown, $q,\dot{q},\ddot{q}_d$ and $\dddot{q}_d$ exists and $\in L_\infty$ and τ_d, $\dot{\tau}_d$, $\ddot{\tau}_d \in L_\infty$. Differentiation of Equation (5) with respect to time and multiplying by M yields the following open loop error system:

$$M\dot{r} = M\ddot{q} - M\ddot{q}_d + M\alpha\dot{e} \quad (6)$$

Modify the open loop error system by substituting for $M\overline{q}$ using the dynamic in (1) and then substituting for $\dot{q}$ using time differentiation of Equation (4) and Equation (5) yields:

$$M\dot{r} = -V_m\dot{q}_d + V_m\alpha e - V_m r - f_d\dot{q} - M\overline{q}_d - \tau_d(t) + \tau + M\alpha\dot{e} \tag{7}$$

We let $\theta = -V_m\dot{q}_d + V_m\alpha e - f_d\dot{q} - M\overline{q}_d + M\alpha\dot{e}$ and rewrite the expression in Equation (7) to form the following open loop error system given by Equation (8). All of the controllers will be designed based on this error system.

$$M\dot{r} = Y\theta - V_m r - \tau_d(t) + \tau \tag{8}$$

3.1 EMK controller

Assuming to have exact knowledge about dynamic of the system, we designed a controller to cancel all the nonlinearities in the system, thus the external disturbance will be the only term left undefined. Considering the error system in Equation (8), we can use a control gain constant matrix (K>0) and design the control torque given by (9) such that the error goes to zero ($e \rightarrow 0$). Substituting this torque in the dynamic yields the closed loop error system given in Equation (10):

$$\tau = -Y\theta - Kr \tag{9}$$

$$M\dot{r} = -V_m r - Kr - \tau d \tag{10}$$

In order to perform the Lyapunov stability analysis, we considering a positive definite (PD), continuously differentiable candidate Lyapunov function given by $V = \frac{1}{2}r^T Mr$. Direct differentiating of this function with respect to time and substituting with the error system in Equation (8), yields:

$$\dot{V} = \frac{1}{2}r^T\dot{M}r + r^T(-V_m r - Kr - \tau_d) \tag{11}$$

Using the skew symmetric property, we can simplify Equation (11) and upper bound it by $\dot{V} \le -K\|r\|^2 - r^T\tau_d$. In the absence of disturbances (τ_d=0), this inequality will reduce to $\dot{V} \le -K\|r\|^2$, which can also be written (by using the expression of the candidate Lyapunov function) as a first order differential equation given by $\dot{V} \le -2KV$ that has the following solution:

$$V(t) \le V(0)\exp\left(\frac{-2Kt}{\lambda_{\max(M)}}\right) \tag{12}$$

It can be concluded from Equation (12), that the system will be globally exponentially stable (GES) by using this controller. We can also observe that $V(t)$ exponentially goes to zero and is $\in L_\infty$, also $\|r\|$ and $\|e\|$ exponentially go to zero and are $\in L_\infty$. Since $Y\theta$ is a function of e and r, it is therefore $\in L_\infty$. As a result, the control input torque (τ) is also $\in L_\infty$. In the presence of disturbances ($\tau_d \neq 0$), the expression for $\dot{V}$ can be upper bounded by $V(t) \le -K\|r\|^2 - c\|r\|$, where c is a positive constant such that $\|\tau_d\| \le c$. In this case, a Globally Uniformly Ultimately Bounded (GUUB) stability result can be concluded where the ultimate bound is given by $\|r\| = \frac{c}{K}$.

3.2 Adaptive controller

The objective of adaptive control was to achieve a trajectory tracking task in the presence of unknown parameters, thus, the controller should be designed based on an estimate of the system model. We proposed the following design for the control torque:

$$\tau = -Y\hat{\theta} - Kr \tag{13}$$

where, K is again a positive control gain matrix and $\hat{\theta}$ represents an estimate of the system parameters. Substituting Equation (13) in Equation (1) yields the following closed loop error system:

$$M\dot{r} = -Y\tilde{\theta} - V_m r - Kr - \tau_d \tag{14}$$

where, $\tilde{\theta} = \theta - \hat{\theta}$ is the difference between the actual and estimated parameters. Differentiation $\tilde{\theta}$ with respect to time gives $\dot{\tilde{\theta}} = -\dot{\hat{\theta}}$ (since θ is assumed to be a constant). In order to design $\hat{\theta}$, we considered a continuously differentiable, positive-definite Lyapunov function candidate given by $V = \frac{1}{2}r^T Mr + \frac{1}{2}\tilde{\theta}^T\Gamma^{-1}\tilde{\theta}$. Differentiating this function with respect to time and substituting for $\dot{\tilde{\theta}}$ with $-\dot{\hat{\theta}}$ and for $M\dot{r}$ with (14) yields:

$$\dot{V} = \frac{1}{2}r^T\dot{M}r + r^T(-Y\tilde{\theta} - V_m r - Kr - \tau d) - \tilde{\theta}\Gamma^{-1}\dot{\hat{\theta}} \tag{15}$$

Using the skew symmetric property to simplify Equation (15) and design $\dot{\hat{\theta}} = -\Gamma Y^T r$, the expression for $\hat{\theta}$ can be then determined by integrating $\dot{\hat{\theta}}, (\hat{\theta} = \int -\Gamma Y^T r dt)$. Substitute $\dot{\hat{\theta}}$ in Equation (15), yields a new expression, $\dot{V} = -Kr^2 - r^T \tau_d$, which can be upper bounded by $\dot{V} \le -K \| r \|^2 - r^T \tau_d$. In the absence of external disturbance, the expression for the upper bound of $\dot{V}$ reduces to $\dot{V} \le -K \| r \|^2$. Since V is a positive definite function and $\dot{V}$ is negative semi definite, we can concluded that $V \in L_\infty$. In addition, V is a function of r and $\tilde{\theta}$, then r and $\tilde{\theta}$ are also $\in L_\infty$. Being r bounded, we have $e, \dot{e} \in L_\infty$, thus $q, \dot{q} \in L_\infty$ which means $Y \in L_\infty$. Also since $\tilde{\theta}, \theta \in L_\infty$, then $\hat{\theta} \in L_\infty$, thus $\dot{r} \in L_\infty$. Therefore, r is continuously differentiable. Since r is square integrable ($r \in L_2$) and uniformly continuous, using the corollary to Barbalat's lemma[15], we can conclude that $r \to 0$ as $t \to 0$ which means that by using this controller, and in the absence of external disturbances, the system is asymptotically stable. In addition, the designed input control torque in (15) is bounded because it is a function of bounded terms. In the presence of a bounded external disturbance, by assuming that $\| \tau_d \| < c$, we will have $\dot{V} \le -K \| r \|^2 - c \| r |$ which results in a GUUB stability result. The ultimate bound can be calculated by setting $\dot{V} = 0$, which yields $\| r \| > \frac{c}{K}$.

3.3 Sliding mode controller

Since the parameters in the model are all unknown, another approach to compensate uncertainties in the system is by crushing them through fast switching, also known as nonlinear robust sliding mode control. This approach comes at the cost of high or even infinite control effort and requires fast switching actuators. For this design, we considered the upper-bounds into the dynamic expressed in Equation (7). We rewrote the error system in Equation (8) by letting $\beta = Y\theta - \tau_d$ which can be upper bounded by $\le c_1 + c_2 \| z \| + c_2 \| z \|^2$, ($z = [e^T \quad r^T]^T$). Therefore, a control torque can be designed given by Equation (16), which yields the closed loop error system in Equation (17). In this design, K is a positive control gain matrix, ρ is a positive constant and $sgn(r)$ is the sign function of r.

$$\tau = -Kr - \rho sgn(r) \tag{16}$$

$$M\dot{r} = -Kr - \rho sgn(r) - V_m r + \beta \tag{17}$$

Considering the continuously differentiable and positive- definite Lyapunov candidate function introduced in the EMK design, by differentiating with respect to time and substituting for $M\dot{r}$ from Equation (17), the following expression for $\dot{V}$ is obtained.

$$\dot{V} = \frac{1}{2} r^T \dot{M} r + r^T (-Kr - \rho sgn(r) - V_m r + \beta \tag{18}$$

Using the skew symmetry property, we can upper bound (18) by $\dot{V} \le -K \| r \|^2 - r^T \rho sgn(r) + r^T \beta$ which can be simplified as $\dot{V} \le -K \| r \|^2$. Solving this differential equation yields a solution of the form $\dot{V} \le -\frac{2K}{\lambda_{\max\{M\}}} V(t)$, where $\lambda_{\max\{M\}}$ gives the maximum eigen value of matrix M. Therefore, we have $V(t) \le V(0) \exp\left(-\frac{2Kt}{\lambda_{\max\{M\}}} \right)$. From this result, it can be concluded GES result for the system. Since $V(t)$ exponentially converges to 0, $\|r\|$ also exponentially converges to 0. Therefore, $\|e\| \to 0$ as $t \to 0$. Because the disturbance was included within the uncertain model, there is no need of any separate stability analysis for a case with disturbance. The constants chosen to squash all the unknown nonlinearities in the system.

3.4 High gain controller

The objective of the torque control design in this approach was to crush the uncertainties in the system through high gain which leads to a high control effort. Using the error system in Equation (8), we designed the control torque as $\tau = -Kr$ where K is a positive control gain matrix. Substituting this control torque in Equation (8) yields the following closed loop error system:

$$M\dot{r} = -Kr - V_m r + \beta \tag{19}$$

Considering the same Lyapunov candidate function as

in the EMK design and its time derivative, and by substitution for $M\dot{r}$ using Equation (19) and applying the skew symmetry property, we can upper bound $\dot{V}$ by $\dot{V} \le -K \| r \|^2 + \rho \| r \|$. It can be seen that $-K \| r \|^2$ dominates $\rho \| r \|$ by large K, and as long as this happens, $V(t)$ will be decreasing. However, because we have $\| r \|^2$, the term $-K \| r \|^2$ will eventually be dominated by $\| r \|$. In the other words, at some point, r will be small enough that $-K \| r \|^2$ will be dominated by $\rho \| r \|$, and since V is a positive definite, radially unbounded and decrescent function, we concluded uniformly ultimate bound stability result. This can be shown by letting $K = k_1 + k_2$ and completing the square term in $\dot{V} \le -K \| r \|^2 + \rho \| r \|$ as follows:

$$\dot{V} \le -k_1 \| r \|^2 - k_2 (\| r \|^2 - \rho \| r \| + \frac{\rho^2}{4k_2^2}) + \frac{\rho^2}{4k_2}$$

$$\therefore \quad \dot{V} \le -C_a V + C_b \tag{20}$$

where $C_a = \frac{2k_1}{M}$ and $C_b = \frac{\rho^2}{4k_2}$. The solution to Equation (20) is $V(t) \le C_a V(0) \exp\left(-\frac{k_1 t}{\lambda_{\max}\{M\}} \right) + C_b$, where $\lambda_{\max}\{M\}$ gives the maximum eigen value of matrix M. Based on this, we can conclude Uniformly Ultimate Bounded (UUB) stability result.

4 Simulation results

The performances of the four designed controller were simulated in the presence and absence of external disturbance. To achieve this aim, each robot link was first modeled as a homogeneous rectangular bar with mass m_i, length l_i, and moment of inertia tensor $J = [I_{xi}\ 0\ 0;\ 0\ L_{yi};\ 0\ 0\ 0\ I_{zi}]$ relative to a frame attached at the center of mass of the link and aligned with the principle axes of the bar. The expressions for the inertia matrix, and the centripetal-Coriolis matrix, $M \in R^{2\times 2}$ in the dynamic model given by Equation (1) were derived by applying the Lagrange's equation known as $(\frac{d}{dt}\frac{\partial L}{\partial \dot{q}_i} - \frac{\partial L}{\partial q_i} = F_i$, where Fi is the external force acting on the *i-th* generalized coordinate) to the two-link manipulator shown in Figure 1 and by calculating the kinetic energy of the manipulator. Letting (x_i, y_i, 0) denote the position of the *i-th* center of mass and r_1 and r_2 to be the distance from the joints to the center of mass for each link, as shown in Figure 1, the kinetic energy is calculated as follows:

$$\begin{aligned} T(q,\dot{q}) &= \frac{1}{2} m_1 (\dot{\bar{x}}_1^2 + \dot{\bar{y}}_1^2) \frac{1}{2} + I_{z1} \dot{q}_1^2 + \frac{1}{2} m_2 (\dot{\bar{x}}_2^2 + \dot{\bar{y}}_2^2) + \\ &\quad I_{z2} (\dot{q}_1 + \dot{q}_2)^2 \\ &= \frac{1}{2} \begin{bmatrix} \dot{q}_1 \\ \dot{q}_2 \end{bmatrix}^T \begin{bmatrix} p_1 + 2p_3 c_2 & p_2 + p_3 c_2 \\ p_2 + p_3 c_2 & p_2 \end{bmatrix} \begin{bmatrix} \dot{q}_1 \\ \dot{q}_2 \end{bmatrix} \end{aligned} \tag{21}$$

where, $\dot{\bar{x}}_1 = -r_1 s_1 \dot{q}_1$, $\dot{\bar{y}}_1 = -r_1 s_1 \dot{q}_1$, $\dot{\bar{x}}_2 = -(l_1 s_1 + r_2 s_{12})\dot{q}_1 - r_2 s_{12} z \dot{q}_2$, $\dot{\bar{y}}_2 = (l_1 c_1 + r_2 c_{12})\dot{q}_1 + r_2 t_{12} z \dot{q}_2$, $s_i = \sin(q_i)$, $s_{ij} = \sin(q_i + q_j)$, $c_i = \cos(q_i)$ and $c_{ij} = \cos(q_{ij})$. Substituting the Lagrangian $L = T$ into Lagrange's equation, the parameters of the M and V_m matrices in the dynamic model (1) become:

$$M = \begin{bmatrix} p_1 + 2p_3 c_2 & p_2 + p_3 c_2 \\ p_2 + p_3 c_2 & p_2 \end{bmatrix}$$

$$V_m = \begin{bmatrix} -p_3 s_2 \dot{q}_2 & -p_3 s_2 (\dot{q}_1 + \dot{q}_2) \\ p_3 s_2 \dot{q}_1 & 0 \end{bmatrix}$$

$$f_d = \begin{bmatrix} f_{d1} & 0 \\ 0 & f_{d2} \end{bmatrix}$$

where, $p_1 = I_{z1} + I_{z2} + m_1 r_1^2 + m_2 (l_1^2 + l_2^2)$, $p_2 = I_{z2} + m_2 r_2^2$, $p_3 = m_2 l_1 r_2$. The calculated numerical values are, p_1 = 3.473 kg·m^2, p_2 = 0.196 kg·m^2, p_3 = 0.242 kg·m^2 corresponding to the link length and weight of the robot, l_1 = 0.024 m, l_2 = 0.16 m and $m_1 = m_2$ = 1.1 kg. In the dynamic model 1, τ_1 and τ_2 represents torque control inputs and q_1, q_2 denotes the angular position of the robot links. The friction term for the simulation was proposed f_{d1} = 5.3 Nm·s and f_{d2} = 1.1 Nm·s. The simulation was performed in MATLAB with the corresponding diagram shown in Figure 2. In order to evaluate the performance of the system, the error and torque in the joint angles in the presence and absence of the bounded disturbance for each designed controller as well as the adaptive parameters estimation were simulated and were plotted through Figures 3-22.

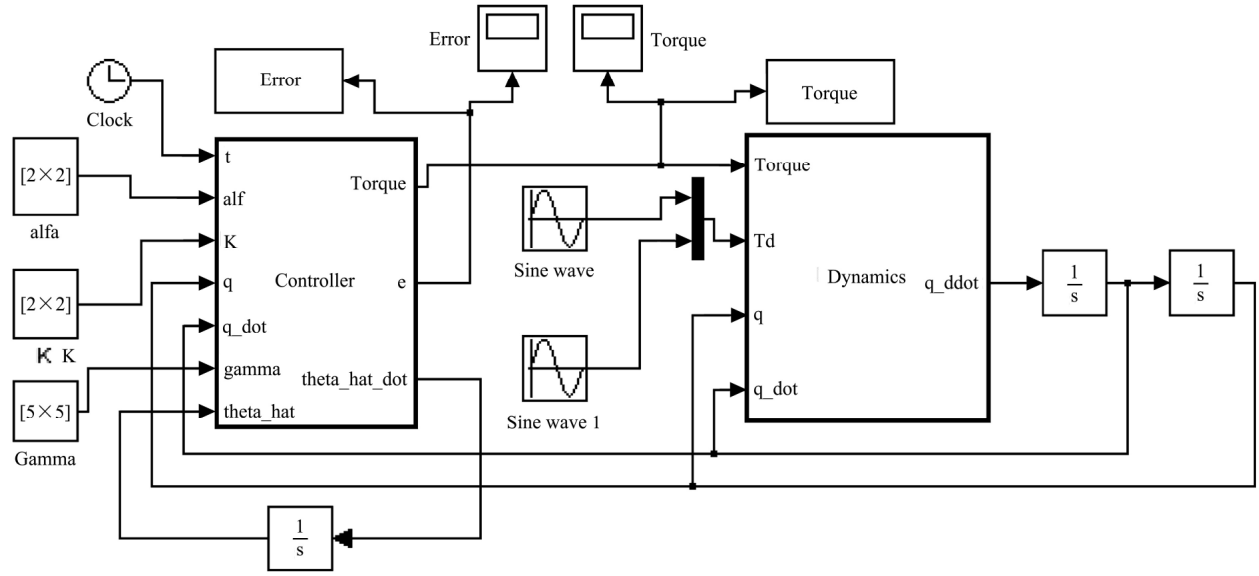

Figure 2 Control simulation diagram with external disturbances

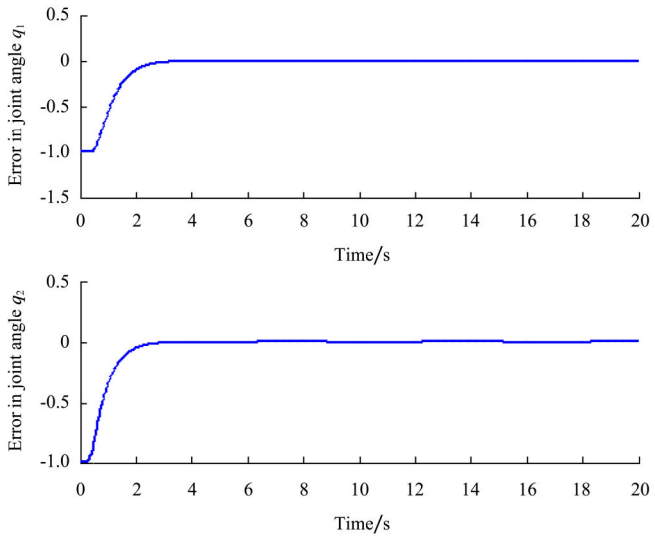

Figure 3 Error plots, EMK controller without disturbances

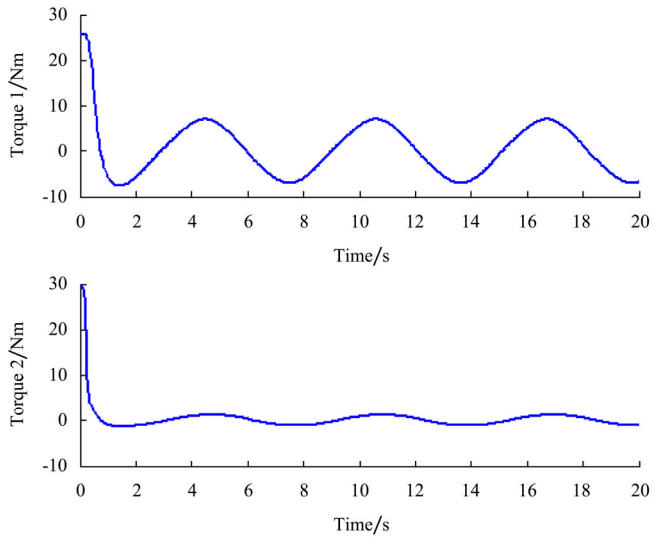

Figure 4 Torque plots, EMK controller without disturbances

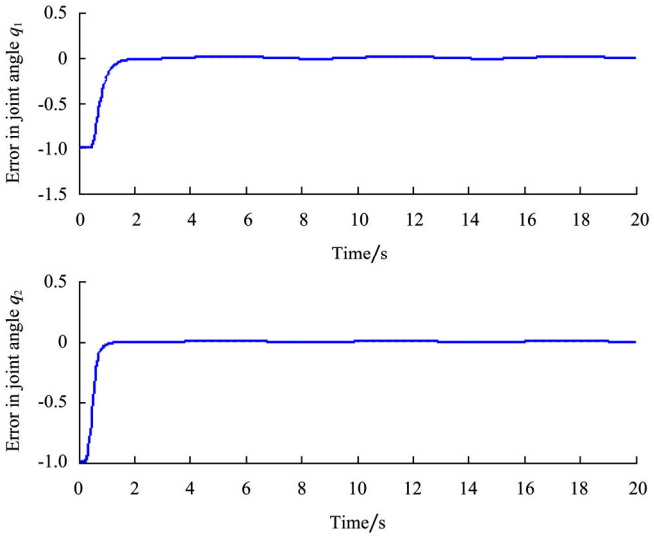

Figure 5 Error plots, EMK controller with external disturbances

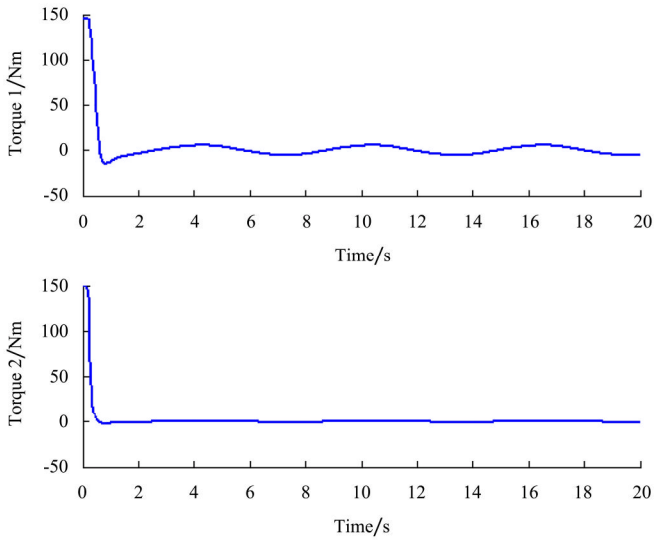

Figure 6 Torque plots, EMK controller without disturbances

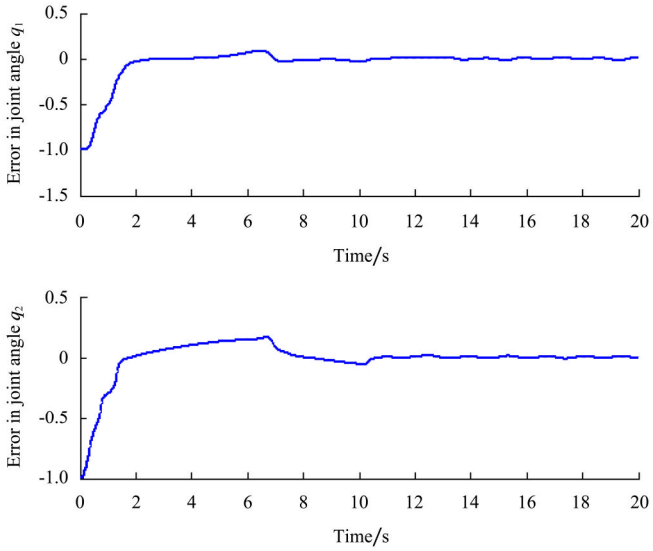

Figure 7 Error plots, adaptive controller without disturbances

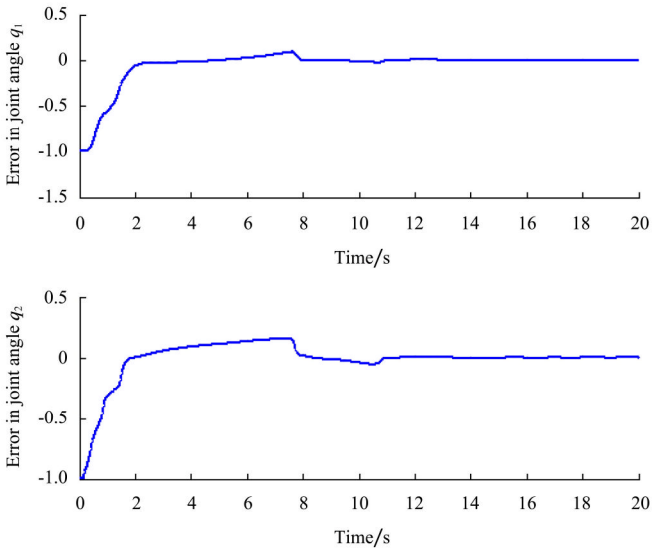

Figure 8 Error plots, adaptive controller with disturbances

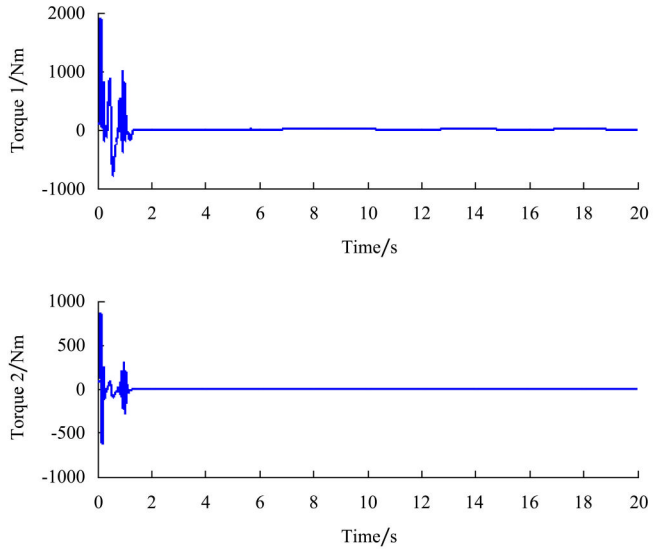

Figure 9 Torque plots, adaptive controller without disturbances

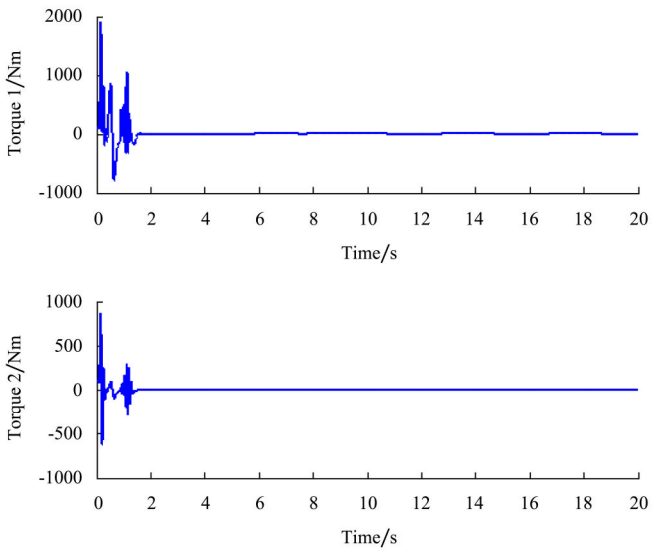

Figure 10 Torque plots, adaptive controller with disturbances

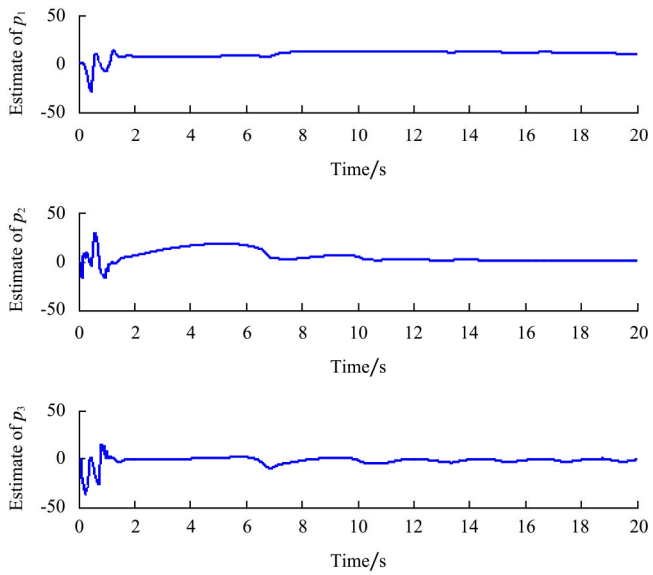

Figure 11 Adaptive estimated parameters, p_1, p_2 and p_3, without disturbances

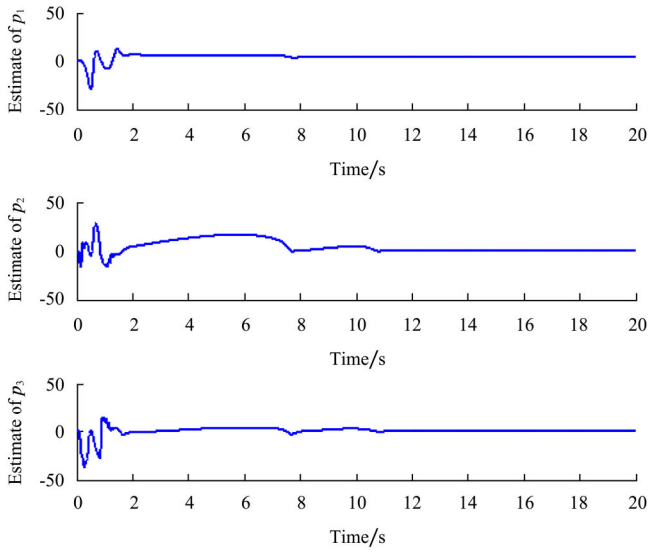

Figure 12 Adaptive estimated parameters, p_1, p_2 and p_3, with disturbances

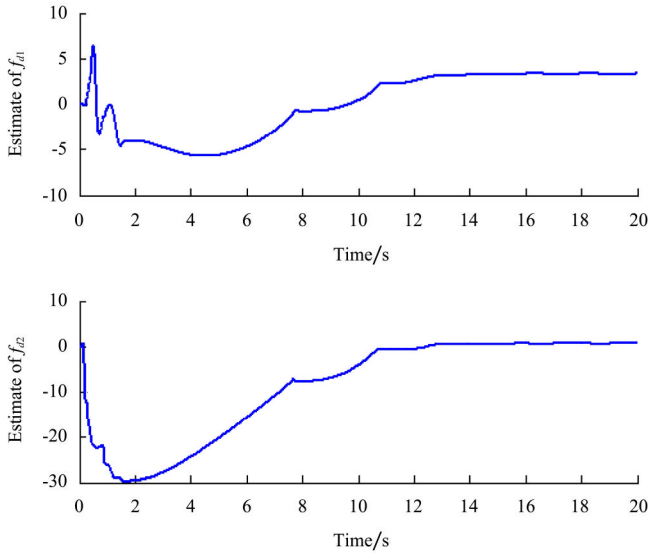

Figure 13 Adaptive estimated parameters, f_{d1} and f_{d2}, without disturbances

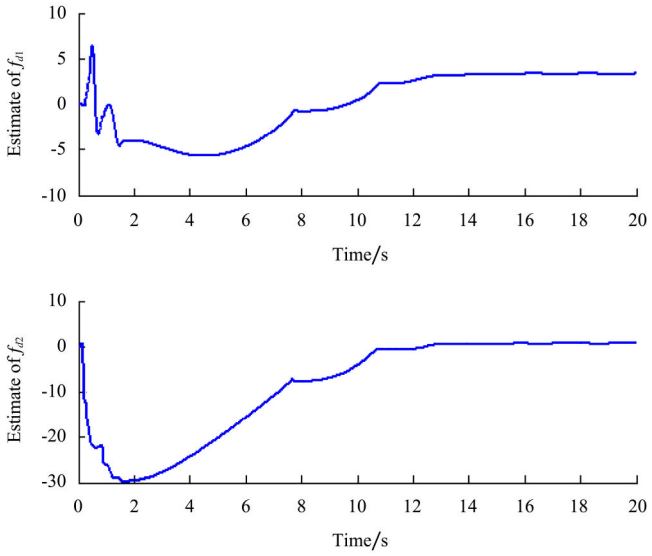

Figure 14 Adaptive estimated parameters, f_{d1} and f_{d3}, with disturbances

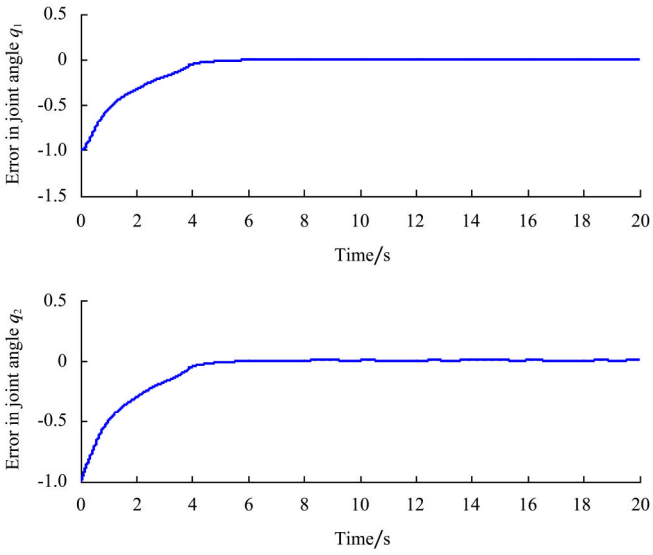

Figure 15 Error plots, SMC, without disturbances

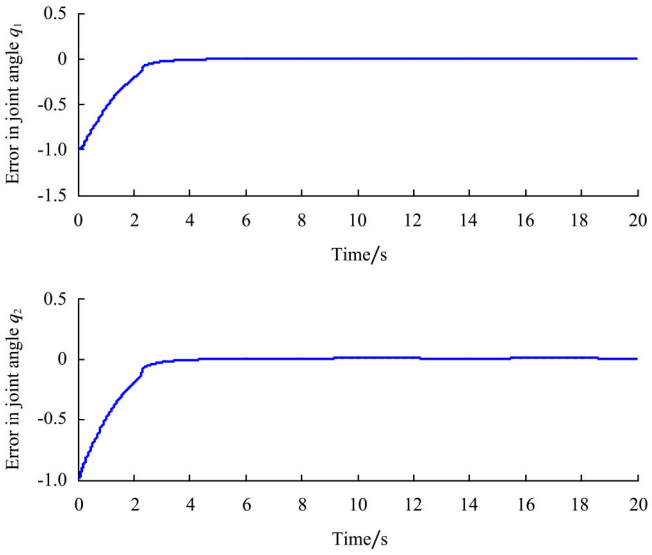

Figure 16 Error plots, SMC, with external disturbances

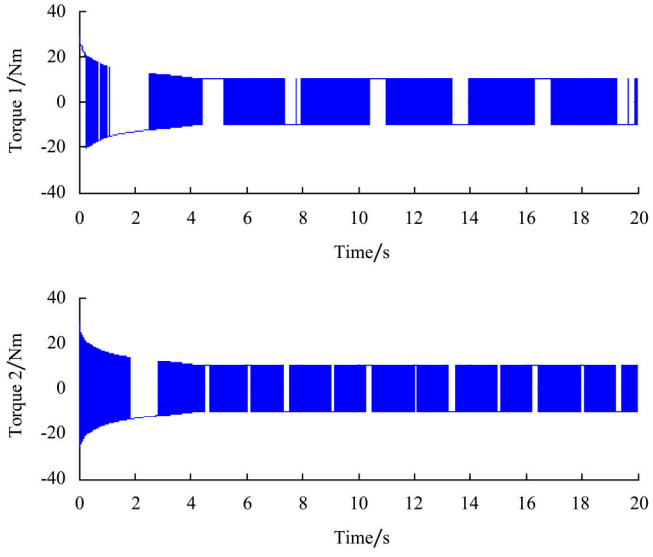

Figure 17 Torque plots, SMC, without disturbances

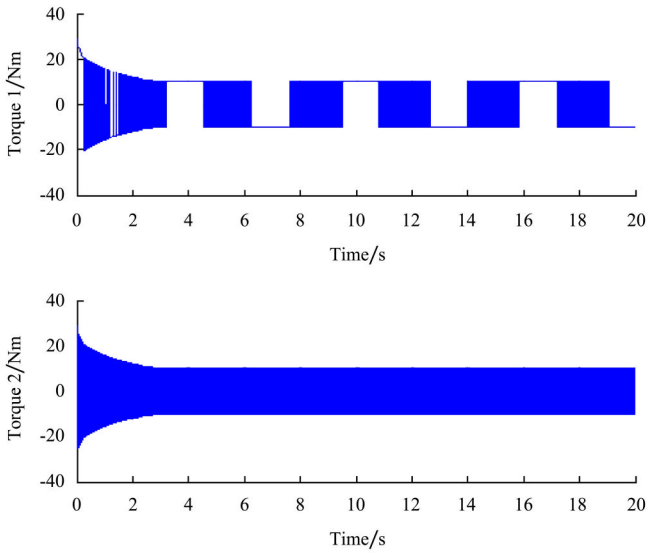

Figure 18 Torque plots, SMC, with external disturbances

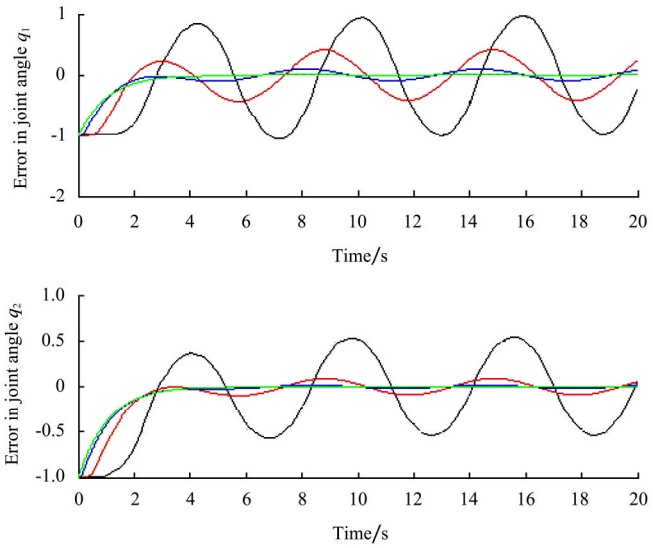

Figure 19 Error plots, high gain controller, without disturbances, (K=1, 10, 50, 500)

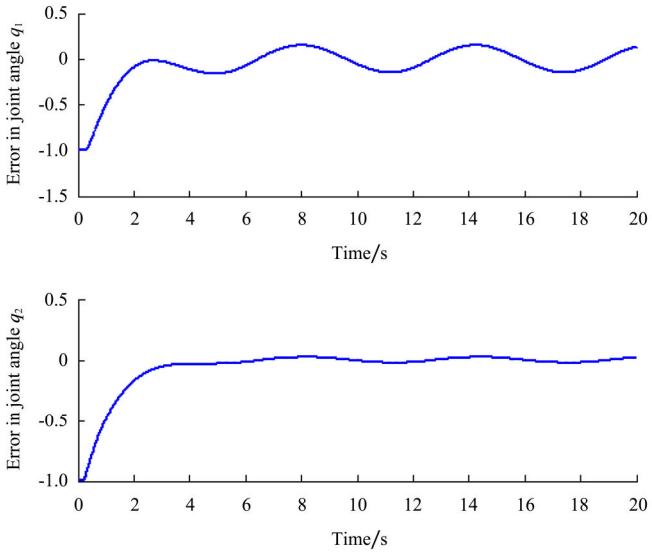

Figure 20 Error plots, high gain controller, with disturbances, K=25

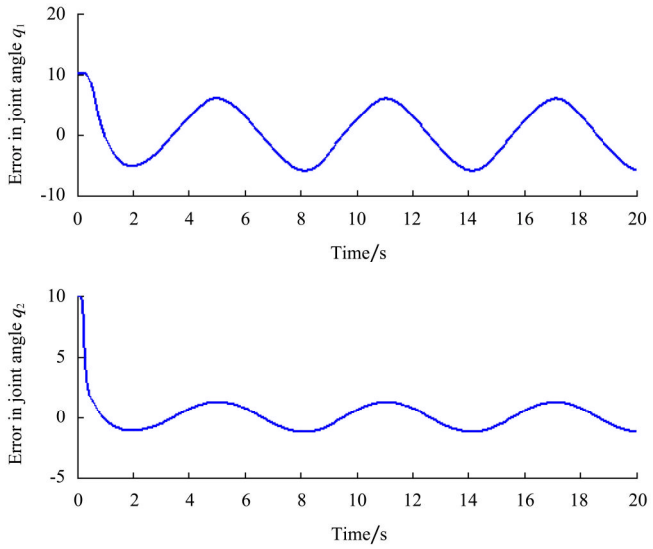

Figure 21 Torque plots, high gain controller, without disturbances, K=10

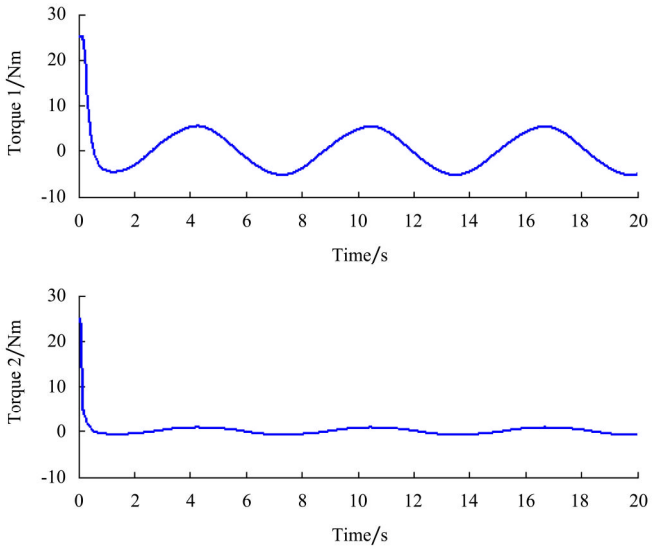

Figure 22 Torque plots, high gain controller, with disturbances, K=25

5 Discussion

Four nonlinear controllers were designed and simulated based on Lyapunov analysis for a two link oil palm harvesting robot manipulator. Exact knowledge of the robot model was assumed in the EMK design in order to cancel the nonlinearities in the system through feedback linearization. A GES result was then obtained. It can be observed from Figure 3 that error exponentially converges to zero when there is no external disturbances to the system. In the presence of unknown, bounded disturbances, as shown in Figure 5, the control torque designed based on the known parameters is not capable of producing exactly zero error result. Therefore, errors converge to a small region and stay within that region. In the other words, not all nonlinearities are cancelled and we have globally ultimately bounded result. It can also be obtained from Figures 4 and 6 that torques are bounded and are in the range of -10 Nm to 30 Nm for the no disturbance case and within a range of -50 Nm to 150 Nm in the presence of disturbance.

To take into accounts the uncertain parameters in the system, it is necessary to use adaptive control to design control torque. As shown in Figures 11-14, the

parameter estimates ultimately reach close to the actual values given by the problem. It can also be obtained from Figures 7 and 8 that the error asymptotically converges to zero in the absence of external disturbances. In the case of having disturbance in the system, the error wiggles around zero, indicating an ultimately bounded stability result. It can also be seen from the torque profiles in Figures 9 and 10 that the torques is within the prescribed limits.

In the SMC design, we can theoretically achieve a GES result, however, as shown in the Figures 15 and 16, it takes a longer time for the error to approximately converge to zero which is because of the discontinuous nature of the controller and since the torque limitations impose constraints on the gain selection. Having upper bounded the unknown dynamics and disturbances by functions of states; the sliding mode controller manages to crush the nonlinearities, however it is not possible to achieve GES when the unknown dynamics cannot be modeled as a function of states, but upper-bounded by a constant. In this case, we can conclude a globally uniformly ultimately bounded stability result. From the torque plots in Figures 17 and 18, we can see that torque has been switching infinitely fast. In the other words, an actuator is required to handle such a bandwidth in order to implement this controller on a real oil palm harvesting robot.

Plots of error for different gains were shown in Figures 19 and 20 for the high gain control design. It can be seen that, as we increase the gain, error gets closer to zero. In reality, increasing gain requires high control effort. One advantage of this controller is its simple design structure which makes it easy to tune and implement. From Figures 21 and 22, it is straight forward to see that the torques patterns applied at the two joints are almost similar to that of the EMK controller, which is because of the adaptation of the system parameters. It can also be observed that the oscillations in torques have been remarkably reduced compared to that in the two previous designs; hence less control energy is required. The controller is robust to the uncertainties in the system, however it only yields a uniformly ultimately bounded stability result.

6 Conclusions

With the mechanization of harvesting, the hard and labor intensive needed in picking and harvesting oil palm in the plantation can be easier, simpler and more important, and it will reduce the manpower shortage problem due to decrease in seasonal labor. In order to successfully achieve this objective, four nonlinear joint angles tracking controllers based on Lyapunov analysis were designed for an oil palm harvesting robot manipulator. The exact model knowledge controller showed the best stability result, compared with all other controllers. It also had the lowest control effort. The problem with this design is the lack of a model that can perfectly describe the system. In addition to that, when disturbances are introduced into the system, the controller will lose its perfect performance and result in a globally uniformly ultimately bounded stability. Adaptive control design was used in order to improve performance. In this design, gains tuning is required to ensure that the control torques are within the actuator limits while maintaining a good tracking performance. Using high gain would come at the cost of increasing control effort, however, it also ensure that any error estimate of the parameters will be compensated. Simulation result showed that the adaptive controller is more efficient especially in the presence of disturbances, in which a GES result was concluded. In the SMC design, the controller provides fast switching action to cancel the nonlinearities and disturbances in the system. This design gave a GES result, however it comes at a high control effort and requires an actuator to switch infinitely fast in time which might inject noise and other disturbances in the system. Because of the discontinuous nature of this controller, tuning of gains is almost useless to archive GES result, which theoretically should have been the case. The high gain controller gave uniformly ultimately bounded stability result in the presence of uncertain model dynamics and bounded disturbances. While EMK controllers cannot handle disturbances at all and adaptive controllers give a GES result, high gain controllers crush the uncertainties at the cost of high control effort. One advantage of this design

was the easiness of the control implementation and gain tuning.

[References]

[1] Pons J L, Ceres R, Pfeiffer F. Multifinger eddextrous robotics hand design and control: a review. Robotica, 1999; 17(6): 661-674.

[2] Mehta S S, Burks T, Dixon W E. Vision-based localization of a wheeled mobile robot for greenhouse applications: a daisy-Chaining approach. Transactions on Computers and Electronics in Agriculture, 2008; 63: 28-37.

[3] Henten E j V, Hemming J, Tuijl B J AV. Collision-free motion planning for a cucumber picking robot. Biosystems Engineering, 2003; 86(2): 135-144.

[4] Kondo N, Ninomiya K, Hayashi S, Ota T, Kubota K. A new challenge of robot for harvesting strawberry grown on table top culture. 2005 ASAE Annual International Meeting; Paper No. 053138. Tampa, FL.

[5] Libing Z, Yan W, Qinghua Y, Guanjun B, Feng G, Yi X. Kinematics and trajectory planning of a cucumber harvesting robot manipulator. Int J Agric & Bio Eng, 2009; 2(1): 1-7.

[6] Monta M, Kondo N, Ting K C. End effectors for tomato harvesting robot. Artificial Intelligence Review, 1998; 12: 11-25.

[7] Kondo N, Monta M, Fujiura T. Fruit harvesting robots in Japan. Advanced in Space Research, 1996; 18(12): 181-184.

[8] Patre P M, MacKunis W, Makkar C, Dixon W E. Asymptotic tracking for systems with structured and unstructured uncertainties. IEE Transaction on Control System Technology, 2008; 16(2): 373-378.

[9] Dixon W E, Zergeroglu E, Dawson D M. Global robust output feedback tracking control of robot manipulators. Robotica, 2004; 22: 351-357.

[10] Liang C, Bhasin S, Dupree K, Dixon W E. A force limiting adaptive controller for a robotic system undergoing a noncontact-to-contact transition. IEE Transaction on control system technology, 2009; 17(6): 1330-1340.

[11] Dixon W E. Adaptive regulation of amplitude limited robot manipulators with uncertain kinematics and dynamics. IEE Transaction on control system technology, 2007; 52(3): 488-493.

[12] Annaswamy A F, Loh A. Adaptive control of continuous time systems with convex/concave parametrization. Automatica, 1998; 34(1): 33-49.

[13] Feemster M, Vedagarbha P, Dawson D M, Haste D. Adaptive control techniques for friction compensation. American Control Conference, 1998; pp 1488-1492.

[14] Spong M, Vidyasagar M. Robot dynamics and control. New York: John Wiley & Sons Inc. 1989.

[15] Sastry S, Bodson M. Adaptive control: stability, convergence, and robustness. Englewood Cliffs, NJ: Prentice-Hall. 1989.